

### Bichromatic wave propagation in periodically poled media

Marek Grabowski

Department of Physics, University of Colorado, Colorado Springs, Colorado 80933

(Received 17 December 1992)

The energy-exchange process between the fundamental and its second-harmonic fields copropagating in an optical medium is facilitated by the spatially periodic dc poling field. The nonlinear dynamics of this system is investigated in the context of an effective Hamiltonian formalism. The explicitly included cross-modulation and self-phase-modulation nonlinear terms lead to the bifurcation instability interpreted as a new switching phenomenon in which both up- and down-conversion efficiencies can be precisely controlled by the external field. Experiments testing predicted effects are suggested.

PACS number(s): 42.65.Ky, 03.50.-z, 42.65.Pc

Many interesting phenomena associated with the propagation of electromagnetic waves in spatially periodic nonlinear media have recently been studied in the context of such diverse branches of physics as nonlinear dynamics [1,2], semiconductor physics [3,4], and nonlinear optics [5,6]. These investigations led to a fairly complete understanding of the regular (periodic), localized (solitons), and chaotic behavior of monochromatic waves in one-dimensional geometries. However, the full picture of spatiotemporal nonlinear phenomena is still missing.

As a first attempt toward understanding the propagation of pulsed classical waves, co-propagating fundamental and second-harmonic fields are studied in the slowly varying envelope approximation, but with an explicit account for nonlinear phase modulation effects [7]. For inversion symmetric systems, such as optical glasses, the energy transfer between the two fields is due to third-order susceptibility and must be mediated by an electric dc field of the appropriate periodicity. This spatially periodic dc field can be either internally self-generated or externally imposed.

Indeed, such a self-generated dc field has been invoked as a possible explanation of a anomalous second-harmonic generation observed in glass optical fibers [8] (for a review see Chap. 10 of Agrawal [9]). This spatially periodic space-charge electric field strongly depends on charge transport, and thus, it is sensitively time dependent. In contrast, Kashyap [5] reported phase-matched second-harmonic generation in externally poled optical fibers, thus allowing much more control over the resulting phenomena. Our approach in this paper is meant to model the latter situation.

We consider the case of two optical fields:  $E_1$  of frequency  $\omega$  and its second harmonic  $E_2$  of frequency  $2\omega$ , copropagating along the  $z$  direction in an inversion symmetric medium poled by a static, spatially periodic electric field  $E_0$ . The coupled propagation equations for these fields follow [6] from the macroscopic wave equation:

$$\begin{aligned}
 (\partial_x^2 + n_1^2)E_1 + \kappa[(E_0^2 + |E_1|^2 + 2|E_2|^2)E_1 \\
 + 2E_0E_2E_1^*] = 0, \\
 (\partial_x^2 + 4n_2^2)E_2 + 4\kappa[(E_0^2 + |E_2|^2 + 2|E_1|^2)E_2 + E_0E_1^2] = 0
 \end{aligned}
 \tag{1}$$

where  $x = z\omega/c$ ,  $\kappa = 12\pi\chi^{(3)}$  measures the nonlinear polarization of the medium, and  $n_j$  stands for the linear refractive index.

To present the main results as elegantly as possible, we find it advantageous to treat Eq. (1) as arising from the following Lagrangian for complex scalar fields with the spatial coordinate  $x$  playing the role of time:

$$\begin{aligned}
 L(E_j, \partial_x E_j) = \sum_{j=1}^2 (|\frac{1}{j}\partial_x E_j|^2 - |n_j E_j|^2) - \kappa V(E_j), \\
 V(E_j) = \sum_{j=1}^2 (E_0^2 + |E_{3-j}|^2 + \frac{1}{2}|E_j|^2)|E_j|^2 \\
 + 2E_0 \text{Re}(E_1^2 E_2^*) .
 \end{aligned}
 \tag{2}$$

In the above equation the nonlinear ‘‘potential’’ contains the external, self- and cross-phase-modulation terms, as well as the term responsible for the dc-field-mediated energy transfer between the fundamental and second harmonic fields.

The Lagrangian of Eq. (2) is globally gauge invariant and the associated conserved current can be identified as

$$J = \sum_{j=1}^2 \frac{1}{j} \text{Im}(E_j^* \partial_x E_j) .
 \tag{3}$$

Clearly,  $\partial_x J = 0$ , reflecting the constancy of the energy flow in the direction of wave propagation. This symmetry of the Lagrangian suggests the use of polar representation for the fields:

$$E_j(x) = \sqrt{P_j(x)/n_j} \exp\{ij[n_j x + \phi_j(x)]\}
 \tag{4}$$

where the fast oscillating components of the fields (those on the scale of wave number  $n_j$ ) have been explicitly separated in preparation for the so-called *slowly varying envelope approximation* (SVE); cf. Ref. [10].

Indeed, for the periodic dc field varying as

$$E_0(x) = \sqrt{\mathcal{E}/n_2} \cos(2n_0 x)
 \tag{5}$$

and with  $n_2 > n_1 \gg n_0$ , the backscattering of the fields by the long-wavelength periodic potential is negligible and the SVE approximation is justified [10]. Consequently, upon substitutions of Eqs. (4) and (5) the SVE Lagrangian becomes

$$L_{\text{SVE}}(P_j, \phi_j, \partial_x \phi_j) = 2 \sum_{j=1}^2 P_j \partial_x \phi_j - \frac{\kappa}{n_1 n_2} H(P_j, \phi_j), \quad (6)$$

$$H(P_j, \phi_j) = P_1 \sqrt{\mathcal{E} P_2} \cos(2(\phi_2 - \phi_1 + \Delta x)) + P_1 P_2$$

where  $\Delta = n_2 - n_1 - n_0$  is the phase mismatch and the second term in the Hamiltonian  $H$  represents the contribution of the self- and cross-phase modulation terms (their significance will be discussed shortly). In addition, we have neglected small terms of the order of  $(n_2 - n_1) \ll 1$  (applicable in most optical materials).

The global gauge invariance of  $L_{\text{SVE}}$  becomes manifest if we introduce new variables—the total and relative phases

$$\phi = 2(\phi_2 + \phi_1), \quad \psi = 2(\phi_2 - \phi_1 + \Delta x). \quad (7)$$

Clearly, under the SVE approximation, the conserved current  $J$  of Eq. (3) is just the total intensity of the propagating fields  $W = P_1 + P_2$ . Using this constancy of  $W$ , and upon further rescaling of the variables as  $p = P_2/W$  and  $\varepsilon = \mathcal{E}/W$ , we arrive at a conservative single degree of freedom system described by an effective Hamiltonian in the relative phase coordinate, with canonically conjugated “momentum”  $p$ :

$$h_\delta(p, \Psi) = \sqrt{\varepsilon p} (1-p) \cos \Psi + (1+2\delta-p)p \quad (8)$$

where  $\delta = n_1 n_2 \Delta / (\kappa W)$  measures the phase mismatch for the energy transfer term.

The equations of motion corresponding to the Hamiltonian of Eq. (8) can be easily written:

$$\begin{aligned} \partial_y p &= \sqrt{\varepsilon p} (1-p) \sin \Psi, \\ \partial_y \Psi &= \frac{1}{2} \sqrt{\varepsilon/p} (1-3p) \cos \Psi + (1-2p) + 2\delta \end{aligned} \quad (9)$$

with the independent coordinate rescaled as  $y = (\kappa W / n_1 n_2) x$ . These equations can be decoupled using the constancy of the Hamiltonian of Eq. (8). In particular, the first-order differential equation for the intensity of the second-harmonic wave becomes

$$(\partial_y p)^2 = Q(p) = \varepsilon p (1-p) - [h_\delta(p_0, \psi_0) - (1+\delta-p)p]^2 \quad (10)$$

with  $p_0$  and  $\Psi_0$  being the initial ( $y=0$ ) intensity and relative phase, respectively. Although the solutions to Eq. (10) can be written in terms of elliptic functions with parameters depending on the roots of the quartic polynomial  $Q(p)$ , these explicit expressions are not particularly informative and shall not be presented here. Instead, we proceed by “graphically” classifying the possible solutions to Eq. (9).

The dynamical system given by Eq. (9) is clearly integrable. Consequently, its phase-space representation proves quite illuminating and it is shown in Fig. 1. Specifically, we restrict our analysis to the perfectly phase-matched propagation, i.e.,  $\delta=0$ . This condition makes the special effects discussed below most pronounced and otherwise it does not change the main conclusions. Clearly, all solutions are periodic. Moreover, for initial conditions restricted to  $\Psi_0=0$  (in phase), the

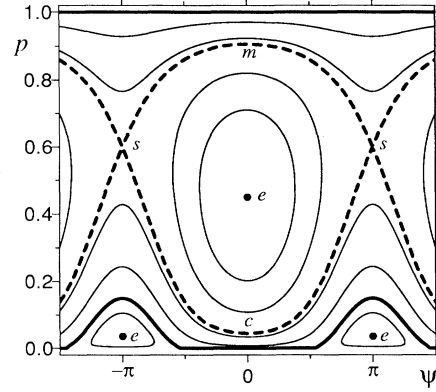


FIG. 1. Representative phase-space trajectories of the solutions to Eq. (9) for  $\varepsilon=0.15$  and  $\delta=0$ . Emphasized are the separatrix (dashed line), zero energy boundary (thick line), and elliptic fixed points (dots).

dynamics of the system resides on non-negative energy manifold ( $h \geq 0$ ) and there are only two types of solutions: librationlike inside the separatrix and rotationlike outside of it. Notice also that the rotationlike solutions exist only due to self- and cross-phase-modulation terms and thus are absent in the usually employed approximations (especially, in the most frequently used undepleted pump approximation; cf. Refs. [5,10]).

Based on Fig. 1, two interesting phenomena can be predicted. For a given strength of the external dc field  $\varepsilon < 1$  and initial conditions:  $\Psi_0=0, p_0 < p_c$ , the second-harmonic intensity oscillates between the initial value of  $p_0$  and the maximum which is limited by  $\varepsilon$  and is always less than  $p_s$  (the saddle point). The period of these spatial oscillations grows from the value of  $2\pi$  at  $p_0=0$ , to infinity at the separatrix  $p_0=p_c$  (solitonlike kink solutions). As the seed intensity  $p_0$  increases past the critical one  $p_c$ , the solutions switch to librationlike, with nearly doubled period and significantly increased-up conversion efficiency up to the maximum as large as  $p_m$  (the upper branch of the separatrix). This is illustrated in Fig. 2, which shows  $p(y)$  for two seed intensities chosen to emphasize the period doubling upon crossing of the separatrix. We shall refer to this behavior as *switching*.

The second type of phenomenon we shall address is *down-frequency conversion*. Since the energy flow direction between the  $\omega$  and  $2\omega$  fields is in itself periodic along the propagation length (with the intensity of the fundamental mode given simply by  $1-p$ ), then for  $p_0 > p_{e0}$  (cf. Fig. 1) one can regard the fundamental mode as a seed for down-frequency conversion. Consequently, similar to the discussion above, the efficiency of the down-frequency conversion switches abruptly upon crossing of the upper branch of the separatrix (i.e., for  $p_0=p_m$ ), and is accompanied by the spatial period doubling. Notice, however, a major difference between up- and down-conversion regimes: for  $p_0=1$ , i.e., for zero initial intensity of the  $\omega$  field, there is no energy exchange between the two fields. This is obviously consistent with the well-known underly-

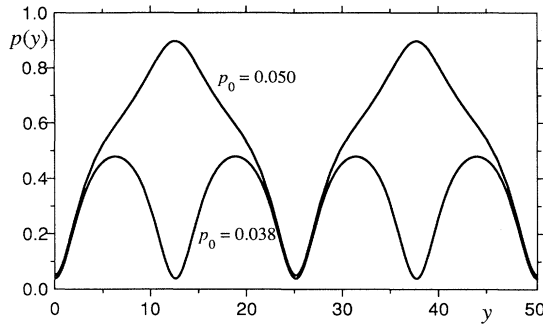


FIG. 2. The intensity of the second-harmonic field as a function of the propagation length for two initial intensities (indicated in the figure) straddling the critical intensity  $p_c = 0.044$  for  $\epsilon = 0.15$ .

ing physics [10] (two high-frequency photons cannot spontaneously combine into a lower frequency one). Nevertheless, this simple fact is missing in models which ignore the nonlinear phase-modulation terms, further emphasizing the importance of the asymmetry attributable to their presence.

It should also be clear that the emergence of the separatrix in the phase space of Fig. 1 represents a truly nonperturbative effect in  $\epsilon$  as can be seen in Fig. 3. All the positive-energy critical points bifurcate from the value of one-half at  $\epsilon = 0$  and then quickly saturate as  $\epsilon \rightarrow 1$ . For the strength of the dc field  $\epsilon > 1$  (not shown in Fig. 3) the saddle point  $p_s$  bifurcates further, and for large  $\epsilon$  the energy transfer term in the Hamiltonian of Eq. (8) dominates the nonlinear phase-modulation terms. Thus, in this limit standard approximation results are recovered. The switching effect is most prominent, however, for small  $\epsilon$  and in particular for  $\epsilon \approx 0.15$ , where the maximum gain on switching reaches a maximum. Consequently, this is the region on which we shall concentrate

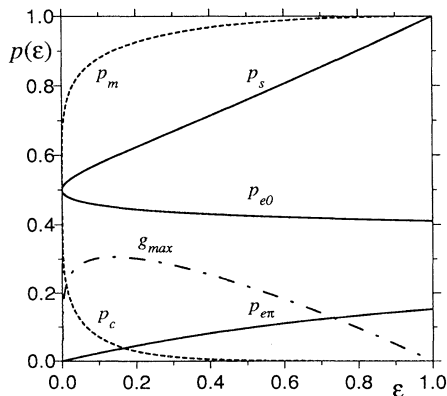


FIG. 3. The characteristic points of the phase space as a function of the dc field's strength. The solid curves represent the saddle ( $p_s$ ) and the elliptic  $\psi = 0$  ( $p_{e0}$ ) or  $\psi = \pi$  ( $p_{e\pi}$ ) fixed points. The broken curves show the critical points:  $p_c$  and  $p_m$ . The dashed-dotted line illustrates the maximum possible gain on switching defined as  $g_{max} = p_m - p_s$ .

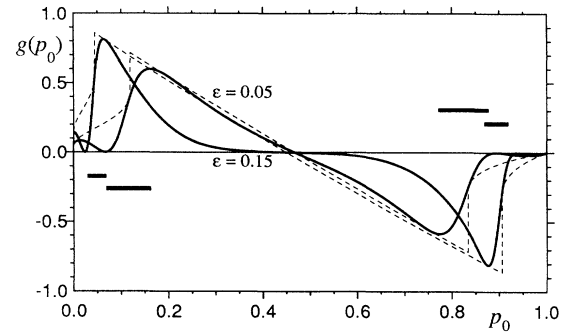


FIG. 4. The up-frequency conversion gain  $g = p(y) - p_0$  as measured at  $y = 3\pi$ , for two values of  $\epsilon$  indicated. The broken line envelopes represent the maximum possible gain while the solid bars indicate the switching regions.

in further discussion.

In practice, one would observe the intensity of the second-harmonic field  $p(L)$ , at a fixed propagation length with  $L$  being the length of the optical fiber or waveguide. In Fig. 4 both of the phenomena defined above are illustrated. The solid curves represent the up-frequency conversion gain as measured at conveniently chosen  $L = 3\pi$ , with the optimal gain shown as dashed curves to serve as a guide to the eye. Notice the dramatic changes of the gain as the seed intensity  $p_0$  is varied. Also, the negative gain for larger  $p_0$  should be interpreted as the above mentioned down-frequency conversion. Although the down- and up-conversion regions appear nearly symmetrical, they are significantly different especially for zero seed intensities: the gain is zero for  $p_0 = 1$  while for  $p_0 = 0$  it is finite and depends on the strength of  $\epsilon$ . The two curves shown in Fig. 4 for two different values of  $\epsilon$  give an indication of how the conversion gain depend on that parameter. Generally, the oscillatory features are sharper for larger  $\epsilon$ , including narrower switching range for both up- and down-conversion regimes. Finally, notice the wide plateau of zero gain for  $\epsilon = 0.15$  and  $p_0$  around the elliptic fixed point reflecting the progressively decreasing im-

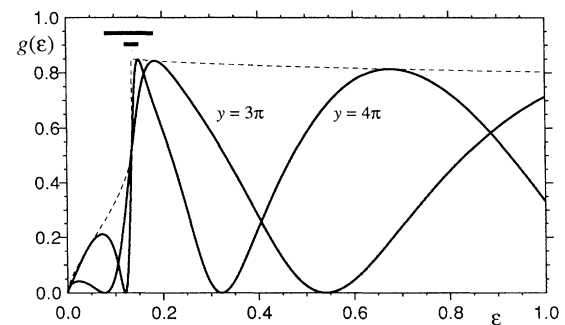


FIG. 5. The conversion gain for seed intensity of  $p_0 = 0.05$  as a function of the dc field strength at two different propagation lengths. The broken line stands for the maximum possible gain and the solid bars indicate the width of the switching region.

portance of the phase modulation terms of libration-like solution for larger values of  $\varepsilon$ .

The switching behavior can also be observed for fixed seed intensity by adjusting the strength of the dc field. This situation is perhaps easier to realize experimentally and is illustrated in Fig. 5. There again the solid curves show the conversion gain (with  $p_0=0.05$  only the up-conversion takes place) as a function of  $\varepsilon$  at different propagation lengths:  $L=3\pi$  and  $4\pi$ . Clearly, the conversion gain is sensitively dependent on propagation length with narrower switching region for larger  $L$  or, since  $L$  scales with the total intensity  $W$ , for higher field intensities.

In conclusion, the nonlinear cross phase modulation that always accompanies the self-phase-modulation in the case of more than one propagating field is shown to be responsible for a novel type of instability. The origin of this instability can be traced to the dynamical bifurcation of the system's fixed points and the emergence of the separatrix isolating different types of periodic solutions. Consequently, the energy exchange between the two

copropagating fields is highly sensitive to all externally controllable parameters: the propagation length  $L$  (or alternatively, total field intensity  $W$ ) set by the sample length, the phase mismatch  $\delta$  controlled by the periodicity of the external static field, the initial seed intensity of the second-harmonic field  $p_0$ , and the strength of the dc field  $\varepsilon$ .

Finally, it should be noted that even though the results are presented in a fairly general context, the phenomena of switching and down-frequency conversion should find exciting applications in the area of integrated optoelectronic devices. Moreover, the findings of this study should encourage the reexamination of the experiments already performed [8,5] on second-harmonic generation in optical fibers.

This work was performed while the author participated in the AFOSR Summer Research Program at the F. J. Seiler Research Laboratory and continued under the AFOSR Research Initiation Grant.

- 
- [1] Marek Grabowski and Pawel Hawrylak, *Phys. Rev. B* **41**, 5783 (1990).
  - [2] François Delyon, Yves-Emmanuel Lévy, and Bernard Souillard, *Phys. Rev. Lett.* **57**, 2010 (1986).
  - [3] D. L. Mills and S. E. Trullinger, *Phys. Rev. B* **36**, 947 (1987).
  - [4] Pawel Hawrylak and Marek Grabowski, *Phys. Rev. B* **40**, 8013 (1989).
  - [5] Raman Kashyap, *J. Opt. Soc. Am. B* **6**, 313 (1989); *Appl. Phys. Lett.* **58**, 1233 (1991).
  - [6] Marek Grabowski (unpublished).
  - [7] Govind P. Agrawal, *Phys. Rev. Lett.* **59**, 880 (1987).
  - [8] Dana Z. Anderson, Victor Mizrahi, and John E. Sipe, *Opt. Lett.* **16**, 796 (1991).
  - [9] Govind P. Agrawal, *Nonlinear Fiber Optics* (Academic, Boston, 1989).
  - [10] Y. R. Shen, *Principles of Nonlinear Optics* (Wiley, New York 1984).